GRADUATE THESIS PROPOSAL

# Local Impacts of Climate Change: Quantifying glacial variation within the Adams watershed in the southern interior of British Columbia


Prepared by:

TAYLOR POWRIE


Prepared for:

MASTER SCIENCE IN ENVIRONMENTAL SCIENCE


THOMPSON RIVERS UNIVERSITY

Supervisor: Dr. Thomas Pypker


January 2023

# Table of Contents

# 1. Introduction

## 1.1 Background

This research will determine any previous shifts in the hydrological regime of the Adams watershed, analyze the past, current, and future dynamics of glaciers located within the watershed, estimate the future contribution of glacier meltwater, and work to address any associated watershed management concerns. Although long-term time series research has been completed to assess the rate of change and influence of glaciers on a broad scale in BC, each sub drainage will be unique in its hydro-ecological response to glacial change due to a variance in extent of glacial coverage, watershed dynamics, and local temperature sensitivities (Pike et al. 2010; Barry and Gan 2022). Limited data has been collected for the glaciers within the Adams watershed, therefore, the actual glacial extent, water equivalence, and potential hydrological influence is unknown.

Hydrological response to glacial change may pose significant ecological and socioeconomical risks depending on basin characteristics, rate of glacier change, as well as cultural and societal utilization of the basin (Spehn et al. 2002; Milner et al. 2009). Adams watershed is a glaciated sub-drainage of the Shuswap watershed that is one of the most important sockeye salmon breeding areas in North America (Henderson et al. 1992; Hume et al. 2003; Kruger and Saayman 2017). The Adams River sockeye run once supported millions of salmon in the upper and lower Adams River; however, the Upper Adams sockeye run was decimated in the early 20$^{th}$ century due to the construction of a splash dam (Hume et al. 2003). There have been reintroduction efforts, as well as nutrient supplementation programs to re-establish a thriving Upper Adams River salmon run, which demonstrates the immense social and economic investment in this watershed (Holmes and Arnouse 2021; DFO 2022).

Understanding the potential impacts of a changing glacial meltwater influence within the Adams watershed hydrological system is integral for ensuring the sustainability of sockeye salmon spawning habitat. Seasonal peak flow associated with glacial meltwater occurs in late summer to early fall, coinciding with the migration and spawning of anadromous fish populations that utilize river systems during this time, including the Adams River sockeye salmon population (Pitman et al. 2020). The continued recession of glaciers may result in less glacial meltwater, reducing the influence of glacial inputs on hydrological systems and shifting watershed hydrology to a precipitation dominated system (Stahl and Moore 2006; Clarke et al. 2015; Pitman et al. 2020; Bevington and Menounos 2022). A precipitation dominated system may be more unpredictable and vulnerable to extreme weather events during the associated salmon spawning period (Pitman et al. 2020; Barry and Gan 2022; Bevington and Menounos 2022).

In distinct watersheds with complex and dynamic hydrological processes, such as the Adams watershed, it is important to first establish if there has been any quantifiable shifts in the historical discharge patterns. Bevington and Menounos (2022) show there has been an increase in the rate of glacier melt in Western Alberta and British Columbia (BC) since 2011 and Li et al. (2018) observed a shift in discharge of an Interior BC watershed due to cumulative effects of forest disturbance and climate variation. With the glaciated headwaters and forest harvesting practices present in the Adams watershed, these cumulative effects should also be observed within the historical Adams River discharge patterns. However, the presence of Adams Lake within the watershed system may buffer any significant changes in the hydrological regime, as it is a large lake (>= 400ha) that has a water holding capacity of ~ 23.2 $km^3$ (GovBC 2022). Observing the characteristics of discharge patterns at the terminus of the Adams watershed will provide insight on the effects of all the interacting factors; therefore, a modified Double Mass Curve will be applied to Lower Adams River hydrometric data to quantify any significant hydrological shifts within the Adams watershed associated with a specific year (Wei and Zhang 2010).

Even in the case of offsetting or buffering factors in the overall drainage area, it is necessary to understand the influence of glacial meltwater, specifically for the Upper Adams River (Milner et al. 2009; Winkler et al. 2010; Chesnokova et al. 2020). Quantifying glacier meltwater directly will work to separate the influence of glaciers on the Adams watershed hydrology from other watershed dynamics (Chesnokova et al. 2020). Glacier meltwater is a factor of climatic inputs that influence glacier mass balance, as well as ice dynamics that are influenced by physical characteristics, such as topography, and ice flow physics. Farinotti et al. (2017) conducted the Ice Thickness Models Intercomparison eXperiment (ITMIX) to compare methods of calculating ice thickness and thus water equivalence. There are many models that require extensive *in situ* data to drive the calculations; however, the Open Global Glacier Model (OGGM) performed well without extensive data (Huss et al. 2010; Farinotti et al. 2017; Maussion et al. 2019). Pelto et al. (2020) described the importance of utilizing Ice Penetrating Radar technology to calibrate calculations within the OGGM, as they found a 38% difference between biased and non-biased ice thickness measurements. This study will apply the OGGM, calibrated with *in situ* ice thickness measurements, to quantify total glacial volume and glacial volume change within the Adams watershed, as well as project glacial run-off contribution to the hydrological system in the future.

## 1.2 Hypothesis and Objectives

The hypothesis being tested include:

1. The glaciers within the Adams watershed are receding.
2. The glaciers within the Adams watershed will have a decreasing input of meltwater in the future based on the IPCC emissions scenerios.
3. The recession of glaciers will influence hydrological processes within the Adams River.

Overall project objectives include:

1. Determine any significant shifts in the historical discharge patterns within the Adams watershed using a modified Double Mass Curve.
2. Quantify the glacier depth and water equivalence of the two largest glaciers in the Adams Watershed with Ice Penetrating Radar.
3. Model glacier evolution and run-off contribution to the Adams River, using the Open Global Glacier Model, based on different climatic forcings simulated by the latest IPCC report, and calibrate model outcomes from *in-situ* ice thickness measurements.
4. Analyze and report on findings in journal articles, a thesis and through public presentations.

## 1.3 Study Area

The Adams River drainage area (Adams watershed) is a sub-drainage of the Shuswap Watershed located in the southern interior of British Columbia (Figure 1). The Shuswap watershed drains into the South Thompson River, which converges with the North Thompson in Kamloops, BC and subsequently flows into the Fraser River Basin (Appendix A). The Adams watershed is the northern most sub-drainage of the Shuswap and contains a majority of the glaciers that may influence the hydrological system of the Shuswap watershed (Figure 1).

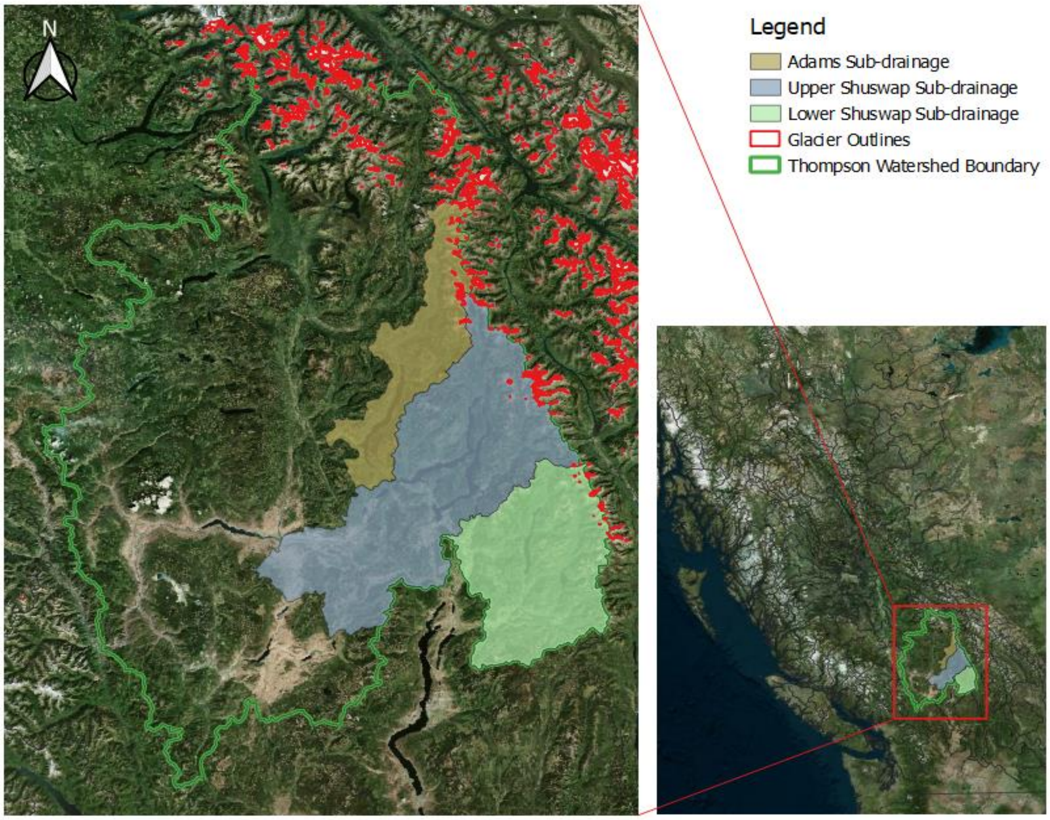


*Figure 1. Location of the Shuswap watershed sub-drainages and glaciers in relation to the broader Thompson drainage basin (BC Data Catalogue 2022; GLIMS 2022).*

The Adams watershed encompasses approximately 286,010 ha of varied terrain, spanning 174 km north to south, and 46 km west to east at its widest point. The headwaters of the watershed are situated within the Columbia mountains and the watershed terminus is located within the southern interior plateau. Due to the elevational and longitudinal difference from north to south, there is a climatic gradient within the watershed. In the northern portion of the watershed, the 1981 to 2010 Canadian Climate Normals report there is an average daily minimum of – 11 °C in the winter and an average daily maximum up to 24.2 °C in the summer, with an average total annual precipitation of 1,124 mm (~720 mm in rain and ~404 mm as snow) (GovCan 2022a)(Appendix B). This northern portion is dominated by Montane Spruce and Interior Cedar-Hemlock biogeoclimatic (BEC) zones. Whereas in the southern portion, the 1981 to 2010 Canadian Climate Normals report an average daily minimum of – 6.6 °C in the winter and an average daily maximum up to 25.8 °C in the summer, with an average total annual precipitation of 739 mm (~515 mm in rain and ~224 mm as snow) (GovCan 2022b)(Appendix C). The lower portion of the Adams watershed is dominated by Interior Cedar-Hemlock an Interior Douglas-fir BEC zones.

# 2. Literature Review

## 2.1 Global Glacier Extent and Status

The cryosphere, or the portion of Earth's water in a frozen state, along with the hydrosphere, atmosphere, biosphere, and the lithosphere make up the five major components of climate systems on earth (Barry and Gan 2022). The cryosphere can be separated into many distinct components; however, glaciers and ice sheets receive the most scientific attention, being the longest lasting form of ice on earth and used to understand historical climatic processes (Kargel et al. 2014; Blunden and Boyer 2021). Ice sheets, including Antarctica and Greenland are large, relatively flat ice masses that flow in all directions, whereas glaciers are smaller ice masses that generally have distinct directional flow lines (Barry and Gan 2022). Although the quantity of ice stored in ice sheets is orders of magnitudes greater, glaciers respond more rapidly to changes in climate; therefore, glaciers are generally utilized for current and future studies of climate change (Zemp et al. 2019; Hugonnet et al. 2021; Barry and Gan 2022; Rounce et al. 2023).

International programs have been established to further understand global ice change, including the World Glacier Monitoring Service (WGMS), that stores standardized data on independent glaciers and ice sheets around the world (WGMS 2021). The WGMS works in close collaboration with the Global Land Ice Measurements from Space (GLIMS) program that collects information on glaciers from satellite imagery, producing the Randolph Glacier Inventory (RGI V6), a global glacier outline inventory (Kargel et al. 2014). Currently, there are over 215,000 glaciers outlined in RGI (V6), encompassing approximately 24,060,000 $km^3$ of fresh water and covering approximately 726,800 ± 34,000 $km^2$ of earth's surface (Kargel et al. 2014; Pfeffer et al. 2014; Barry 2016; Rounce et al. 2023).

Each glacier will have a distinct response to local climate based on factors of topography (e.g., aspect, slope, elevation, basal substrate, and shading features), climatic factors (e.g., wind dispersal of snow, precipitation, and local temperature), and physical factors (e.g., avalanches and surface sedimentation); however, there is a general homogenous response of global glacier recession directly related to global annual temperature rise (Rounce et al. 2023). On a planetary timescale, global climate is a function of solar main sequence brightening, atmospheric composition as a result of biological processes and geological controls, and earth rotation variations (i.e., obliquity and eccentricity) (Kargel et al. 2014). These climatic factors have impacts on global temperature at timescales of $10^4$ to $10^9$ years and have largely driven the long-term glacial cycles (i.e., the ice age and the little ice age) (Kargel et al. 2014). Arrhenius (1896) contributed to our understanding of planetary cycles when he calculated the warming potential of $CO_2$ in the atmosphere. In 1908, Arrhenius suggested that a rise in global temperature of 5-6 °C, directly related to doubling the atmospheric contributions from industrial emissions, would ensure our fate was not met by a new ice age (Arrhenius 1908). However, over the last century, we have observed the potential impacts of increasing anthropogenic $CO_2$ emissions, and the adverse impacts associated with climate change, including the deleterious effects of the planets receding frozen water reservoirs (IPCC 2021).

Rounce et al. (2023) ascertained that glaciers in all regions of the world are experiencing a net decrease in area and mass, linearly related to mean annual temperature rise, reducing freshwater storage and increasing mean sea-level rise. Zemp et al. (2019) found that glacial recession contributed 27 ± 22 millimeters to global mean sea-level rise between 1961 to 2016. In addition, based on current projections of temperature increases (+ 2.7 °C), global glacier recession is projected to contribute another 115 ± 44 millimeters to mean sea-level rise from 2015 to 2100 (IPCC 2021; Rounce et al. 2023). In regard to freshwater storage, 49 ± 9 to 83 ± 7 % of glaciers are projected to disappear by 2100, varied dependent on the different IPCC climate scenarios (Rounce et al. 2023). The rate and timeframe in which glaciers are projected to disappear differs on global region, with regions of smallest glacier mass being the most sensitive to mean global temperature rise, including Western Canada and USA (Rounce et al. 2023).

As glaciers recede on a regional scale, it has been proposed that hydrological flow originating from glaciers will be influenced relative to the glacial state of pre or post peak flow (Stahl and Moore 2006; Pradhananga and Pomeroy 2022). In the pre peak-flow phase, pro glacial basins will experience an increased flow rate due to an increased rate of glacial melt; whereas, in the post peak-flow phase, pro glacial basins will experience a decreased flow rate, due to a decrease in glacier extent (Stahl and Moore 2006). These shifts in the hydrological regime may be observed on three different time-scales, impacting the long-term (decadal), intermediate-term (seasonal), and short-term (diurnal) storage and discharge of water (Jansson et al. 2003). As glaciers progress into the post peak flow phase, glacial river basins will shift from an energy supply to precipitation supply dominated hydrology, altering flow regimes at all time-scales and increasing susceptibility to extreme hydrological events (i.e., floods and droughts) (Milner et al. 2009). Further potential changes associated with shifts in glacial contribution to stream hydrology include higher stream temperatures, variability in suspended sediment fluxes and concentrations, as well as altered water chemistry (Moore et al. 2009). These effects of glacier recession driven by anthropogenically caused climate change will impact communities and ecosystems on a global, regional, and local scale.

## 2.2 Glaciers in North America

Glaciers in North America (NA) are constrained to the western side of the continent, with a majority of glacier coverage occurring above the 49th parallel (Figure 2) (Moore et al. 2009).

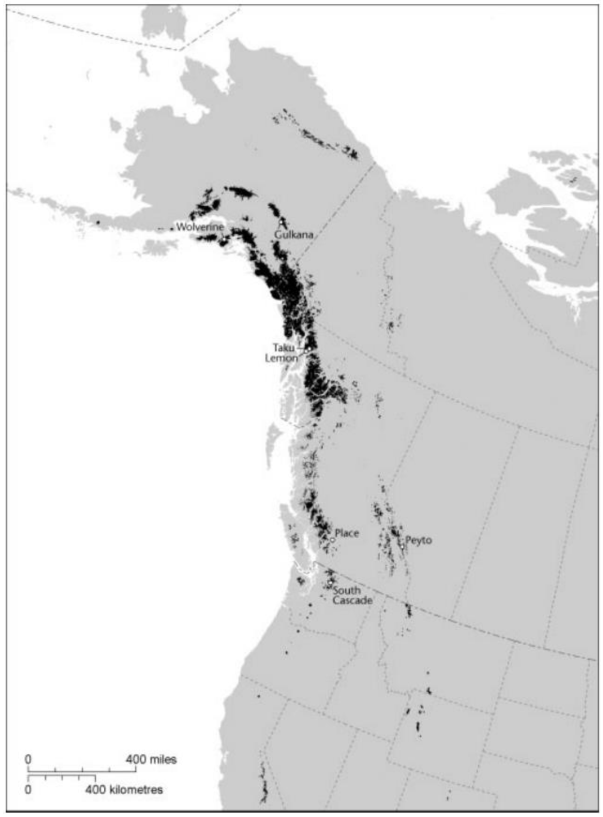


*Figure 2. Glacier coverage in North America based on 2008 imaging (Moore et al. 2009).*

Contemporary North American glaciers are predominantly controlled by decadal climate patterns influenced by oceanic currents (Kargel et al. 2014). The principle component of climatic influence on glaciers in NA is the Pacific Decadal Oscillation (PDO) (Moore et al. 2009; Kargel et al. 2014); however, there are other underlying processes that influence North American glacier change to a lesser degree, including the El Nino Southern Oscillation (ENSO), the North Atlantic Oscillation (NAO), and the Arctic Oscillation (AO). These climate patterns result in variable rates of glacier expansion or recession over variable time frames. Arendt et al. (2002) estimated a total annual volume change of -52 +/- 15 $km^3$ $yr^{-1}$ (water equivalent) for glaciers in Alaska between the mid-1950's to mid-1990's and a total annual volume change of -96 +/- 35 $km^3$ $yr^{-1}$ based on repeated measurements of the same glaciers between mid-1990's to 2001. Jacob et al. (2012) completed mass change calculations of glaciers in Alaska between 2003 to 2010 and found a total annual volume change of -46 +/- 7 $km^3$ $yr^{-1}$. Although, there is variability in the rate of glacier change over time, there has been a continuous trend of glacial recession in NA since the little ice age (Moore et al. 2009; Bevington and Menounos 2022).

The trend of glacier recession is forecasted to continue, as recent projections suggest that the Western Canada and USA region is one of the most globally sensitive regions to glacier recession (Rounce et al. 2023). Glaciers in Western Canada and USA are projected to lose 60 – 100% of their mass by 2100 based on a 1.5 to 3 °C mean global temperature increase (Rounce et al. 2023). Recession of this magnitude will have immense implications for renewable energy, recreation, community water utilization, and aquatic ecosystems.

## 2.3 Local Context

In British Columbia (BC) alone, glaciers cover approximately 3% of the landmass, measured at a total area of 28,233 $km^2$ in 1985 and 25,218 $km^2$ in 2005 (Bolch et al. 2010). Utilizing remote sensing techniques, Bevington and Menounos (2022) observed that glacier recession in BC and Alberta has accelerated since 2011 relative to 1984 - 2010 rates, increasing from - 49 ± 7 $km^2$ $y^{-1}$ over 1984–2010 to 340 ± 40 $km^2$ $y^{-1}$ over 2011–2020, a sevenfold increase across the study area (Bevington and Menounos 2022). The advent of remote sensing techniques in glaciological studies has increased our capacity to observe and predict glacial processes over large areas; however, these techniques can also simplify the complexities of glacial dynamics and mass balance, resulting in errors in measurements that are necessary to reduce when observing impacts of glacial melt on a watershed-scale.

Glacial melt is a direct result of net negative mass balance of glaciers. Mass balance is the ratio between the accumulation zone and ablation zone of a single glacier over time, dependent on precipitation and energy inputs (Figure 3) (Cogley et al. 2011). Glacial ice is formed when snow is compressed under accumulating surface layers of solid precipitation, forming firn and eventually ice, as air between firn crystals is forced out (Barry and Gan 2022). For glaciers to accumulate mass, it is necessary for surface snow layers to persist throughout the year. The area of the glacier in which surface snow persists in a given year is designated as the accumulation zone, whereas the area in which surface snow does not persist in that given year is the ablation zone. The accumulation zone will have a net gain in mass over a given year while the ablation zone will have a net loss, and the mass balance is the difference in mass gained and lost between these two zones (Cogley et al. 2011; Barry and Gan 2022). An overall positive mass balance will cause the glacier area to expand, and a negative total mass balance will cause the glacier area to shrink. Remote sensing techniques, specifically satellite imagery analyses, rely on surface mass balance ratios and glacier area to determine rate of glacial change, as well as to extrapolate glacier volume and water equivalence (Kargel et al. 2014; Maussion et al. 2019); however, this may overlook the complexities of internal and basal mass balance processes of distinct glaciers (Figure 3).

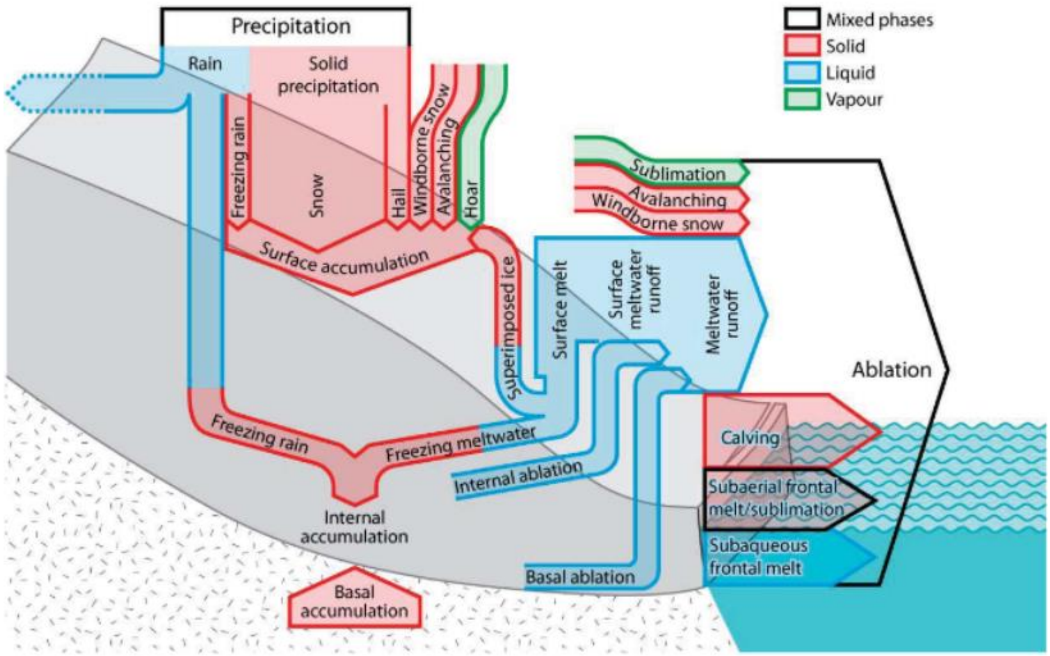


*Figure 3. Mass balance components of a glacier (Cogley et al. 2011).*

Glacier ice deforms overtime due to internal pressures and gravitational forces (Cuffey and Paterson 2010). The velocity of deformation varies throughout the glacier dependent on factors of friction, slope, basal topography, ice density, and ice depth; therefore, each glacier will have unique flux patterns, transferring ice downslope at varying rates (Cuffey and Paterson 2010). Ice dynamics, or the internal movement of ice, will determine the evolution of ice thickness, and thus glacier volume over time. As glacier run-off is a function of ice density and change in volume over time, it is essential to quantify glacier evolution in the Adams watershed to predict the influence glaciers will have on the hydrological system.

The best way to assess internal mass turnover in a glacier is through direct observations and *in situ* measurements; however, these methods are not always feasible due to hostile environments, physical barriers, and lack of long-term baseline data. Glacier models are thus utilized to distill key components down based on previous knowledge of glacier physics (Farinotti et al. 2017). Initial ice thickness is necessary to drive glacier evolution models and direct ice thickness measurements are sparce; therefore, many different computations have been developed to estimate initial ice thickness (Farinotti et al. 2017; Pelto et al. 2020) In this project, we will utilize a mass conservation approach that assumes the ice flux divergence has to be compensated by the rate of ice thickness change (i.e., height of the glacier) and mass balance, as mass cannot be created nor destroyed (Cogley et al. 2011; Maussion et al. 2019). We will model ice flux utilizing estimated glacier flowlines and previous understanding of glacial physics and integrate direct mass balance from surrounding glaciers in close proximity to the Adams watershed to compute ice thickness change (Maussion et al. 2019). We will also integrate direct measurements of ice thickness from two representative glaciers within the watershed to calibrate the model for increased precision (Pelto et al. 2020).

# 3. Methods

## 3.1 Modified Double Mass Curve

Double Mass Curves in hydrology are used to compare the discharge of two distinct watersheds: a control and a study watershed that has been altered by a treatment or disturbance (e.g., logging or natural forest disturbance) (Searcy and Hardison 1960). However, in this study a modified Double Mass Curve (mDMC) developed by Wei & Zhang (2010) is used to analyze discharge of a single watershed, where in theory, with all other factors remaining constant, effective precipitation within the Adams watershed should be linearly associated with the actual observed quantity of discharge (Wei & Zhang, 2010). Based on this assumption, a difference between effective precipitation and actual discharge within a single watershed DMC can be associated with a shift in hydrological dynamics due to factors other than a change in precipitation inputs.

### 3.1.2 Effective Precipitation vs Accumulated Annual Discharge

Effective precipitation for a watershed is calculated as the difference between precipitation and actual evapotranspiration, as long-term groundwater storage has been found to have a negligible net impact on watershed hydrological dynamics (Wei and Zhang 2010). Climate data was extracted from ClimateBC (v7.31) from 1980 – 2021, gridded to suit elevation throughout the Adams watershed, and used to calculate average annual (hydrological year) precipitation. Actual evapotranspiration is calculated in a three-step process, using an equation for extraterrestrial radiation (Equation 1), Hargreaves equation for potential evapotranspiration (Equation 2), and Zhang's equation for actual evapotranspiration (Equation 3) (Hargreaves and Samani 1982; Campbell and Norman 1998; Zhang et al. 2001). Annual precipitation and annual actual evapotranspiration values were then converted to $m^3$/year and multiplied by the area of the watershed before proceeding with the final calculation of effective precipitation, being the difference in the two annual measurements.

Extraterrestrial Radiation:

$$S = \left[0.3(1-\tau^{m})S_{po}cos\Psi\right] + [S_{po}cos\Psi] \qquad [\ \textit{Equation 1}\ ]$$

where $S$ is solar radiation (W m$^{-2}$), $\tau$ is atmospheric transmittance, $m$ is optical air mass number, $S_{po}$ is extraterrestrial flux density (W m$^{-2}$), and Ψ is the zenith angle (radians) (Campbell & Norman, 1998).

Hargreaves equation:

$$E_0 = 0.0023(Ra)\left[\frac{(T_{max}+T_{min})}{2} + 17.8\right](T_{max} - T_{min})^{0.5} \qquad [\ \textit{Equation 2}\ ]$$

where $Ra$ is extraterrestrial radiation (mm day$^{-1}$), $T_{max}$ is maximum monthly temperature (°C), and $T_{min}$ in monthly minimum temperature (°C) (Hargreaves & Samani, 1982).

Zhang's equation:

$$E = \frac{P[1+\omega\left(\frac{E_0}{P}\right)]}{[1+\omega\left(\frac{E_0}{P}\right)+\left(\frac{P}{E_0}\right)]} \qquad [\ \textit{Equation 3}\ ]$$

where $E$ is actual evapotranspiration (mm), $\omega$ is a vegetation factor, $P$ is precipitation in (mm), and $E_0$ is potential evapotranspiration (mm) (Zhang et al., 2001).

Accumulated annual discharge is the sum of all daily discharge quantities throughout the hydrological year (October 1 – September 30). Hydrometric data from the Adams River station near Squilax (Station number: 08LD001) was acquired from Environment Canada Water Office from 1980 – 2021. To produce a mDMC, accumulated annual discharge is plotted against accumulated annual effective precipitation for each watershed with an expected linear relationship. Any breaking point (i.e. a shift or bend in the curve), would be indicative of a shift in watershed discharge. The area between the curve and a projected straight line may be associated to factors aside from precipitation inputs.

### 3.1.3 mDMC Statistical Analysis

An Auto-Regressive Integrated Moving Analysis (ARIMA) model, will be used for the statistical analysis of the mDMC with an intervention analysis extension. ARIMA models are applied to time series data with a non-stationary mean (i.e., a mean that changes over time with all else equal) (Wei 2006). The intervention analysis is responsible for incorporating exogenous forces into a time series analysis that cause a single point step (Box and Tiao 1975). To do so, an ARIMA is applied to the time series data prior to the intervention point (i.e., break in the linear trend) and predicted values are generated for post intervention. The difference between the actual observed values and the predicted values are then computed (Box and Tiao 1975; Wei 2006; Wei and Zhang 2010). The ARIMA model is necessary, as it has the capacity to determine the statistical significance of the step change while accounting for autocorrelation (Rodionov 2005; Wei and Zhang 2010).

## 3.2 Open Global Glacier Model

The Open Global Glacier Model (OGGM) is an open-source model that can be utilized to analyze current and future glacier evolution and melt dynamics (Maussion et al. 2019). The OGGM is well suited for this study as it performs well in quantifying alpine glacier parameters amongst models that do not require extensive *in situ* data (Farinotti et al. 2017; Pelto et al. 2020). Furthermore, the OGGM is built with a modular design, with ordered tasks being applied to a single glacier or a set of glaciers. This design allows for input options during each distinct task based on considerations of data availability and computational resource accessibility, as well as accuracy of boundary conditions estimations (Maussion et al. 2019). With this design, any *in situ* data collected (e.g., initial glacier thickness) can be utilized to update and calibrate the model.

The OGGM includes five distinct modules that will be used within this study, including i) preprocessing, ii) flowlines and catchments, iii) climate data and mass balance, iv) ice thickness, and v) ice dynamics. Available local climatic data, ice thickness measurements, and nearby mass balance observations will be used to update the regional specificity of the OGGM model, otherwise the model default values are used where suggested. Detailed description and documentation of the model can be found in Maussion et al. (2019) and online (http://oggm.org).

### 3.2.1 OGGM Preprocessing

The preprocessing module involves acquiring accurate glacier outlines, a local gridded map, and topographical data. The glacier outlines are retrieved from the Randolph Glacier Inventory (RGI V6; Pfeffer et al. 2014) and corrected to represent current glacier areas by utilizing a Bing aerial base map and SENTINAL-2 false colour imaging. The resolution of the local gridded map is a function of glacier area with $dx = aS^{1/2}$, where dx is the local map resolution, a is 14, and S is the area of the glacier in $km^2$. The minimum resolution bound is 10m and the smallest glacier within the Adams watershed is less than 0.5 $km^2$; therefore, a local gridded map of 10m resolution is used. As the Adams watershed is within the 60 ° S – 60 ° N range, the OGGM will automatically choose the Shuttle Radar Topography Mission (SRTM) topographical data for this area (Jarvis et al. 2008; Maussion et al. 2019).

### 3.2.2 OGGM Flowlines and Catchments

Glacier flowlines are the foundation for all subsequent modules in the OGGM. The OGGM flowline computations are based on an adapted Kienholz et al. (2014) algorithm that defines a main stem of a glacier with the ability to add multiple additional tributary branches. Once each flowline is fit to the local topography and tributary area of the designated glacier, each flowline branch is appointed a Strahler number which will guide the glacier evolution within the model by forcing tributaries to flow into the main stem. The number of flowlines, the spacing of the flowlines, and the catchment area associated with each flowline will be a function of the size and shape of the specific glacier, as well as the resolution of the local gridded map. Although the flowlines for each glacier will be unique in nature, the process to compute each glacier's flowline is consistent and methods are directly followed as outlined in Maussion et al. (2019).

### 3.2.3 OGGM Climate Data and Mass Balance

Mass-balance measurements for the glaciers within the Adams watershed are necessary to be able to model future ice dynamics, and thus glacier melt rates. The OGGM utilizes a combination of regional gridded climatic data, as well as direct observations of representative glaciers to estimate monthly mass balance with the following equation:

$$m_i(z) = p_f P_i^{Solid}(z) - u^* \, max(T_i(z) - T_{Melt}, 0) + \varepsilon \qquad \text{[ \textit{Equation 4} ]}$$

where $m_i$ is monthly mass balance at elevation $z$, $p_f$ is a global precipitation correction factor extracted from the nearest Climate Research Unit (CRU), defaulted to 2.5 in OGGM (Maussion et al. 2019; Harris et al. 2020), $P_i^{Solid}$ is the monthly solid precipitation, $u^*$ is the glacier's temperature sensitivity, $T_i$ is the monthly air temperature, $T_{Melt}$ is the monthly air temperature at which ice melt is assumed to occur, and $\varepsilon$ is a bias correction term.

For the temperature sensitivity parameter ($u^*$), Marzeion et al. 2012 developed a method to incorporate glacier-specific conditions into a mass-balance estimation. To conduct this method, direct observations of specific mass balance from surrounding glaciers are necessary. The World Glacier Monitoring System (WGMS) has a list of 254 acceptable glaciers with accessible data to use for this purpose through the Fluctuation of Glaciers database; however, the closest glaciers to the Adams watershed within this database are Peyto glacier in the Canadian Rockies, Place glacier in the Coast Mountains, and the Columbia glacier in Mt Baker-Snoqualmie National Forest, located in the United States. For more accurate assessments of regional specific mass balance, values from Nordic Glacier (approximately 90 km east of the Adams watershed glaciers) and Zillmer glacier (approximately 80 km northwest of the Adams watershed glaciers) will be used. Pelto et al. (2020) observed specific mass balance at these glaciers from 2014-2018 (Nordic) and 2013-2018 (Zillmer) and utilized these observations within the OGGM framework to correct bias in estimates of glacier thickness within the

Columbia drainage basin. The direct measurements of specific mass-balance play a minor role in the temperature sensitivity process; however, they are important for defining the model uncertainty (Maussion et al. 2019).

### 3.2.4 OGGM Ice Thickness

OGGM computes ice thickness through a mass conservation approach closely related to the method developed by Farinotti et al. (2009). This method is based on the previous calculations of mass balance and physics of ice flow (i.e., ice velocity and ice flux) applied to flowlines on distinct glaciers. The base equation for this computation is:

$$q = uS \qquad [\ \textit{Equation 5}\ ]$$

where $q$ is the ice flux ($m^3\ s^{-1}$) through a glacier cross section of area $S$ ($m^2$), and $u$ ($m\ s^{-1}$) is the average ice velocity. Local ice thickness (m) can be computed by finding the square root of the associated local $S$. Finding ice thickness therefor necessitates that $q$ and $u$ are known. The depth-integrated ice velocity ($u$) is computed using a shallow-ice approximation approach developed by Hutter (1983) and described by Maussion et al. (2019). The ice flux ($q$) calculation relies on mass balance measurements as estimated in the previous module and assumes a steady state where apparent mass balance is equal to our estimated mass balance (Maussion et al. 2019).

Maussion et al. (2019) suggest there is an option to include a basal sliding parameter into the calculation of ice velocity ($u$); however, due to the complexity of the terrain throughout the Adams watershed, the sliding velocity parameter will be set to zero, transferring all uncertainty in basal sliding to the creep parameter ($A$) that is accounted for in both equations of $q$ and $u$ (Glen 1955; Pelto et al. 2020). Finding the optimal $A$ ($A_{opt}$) is critical, as local thickness and total glacier volume are very sensitive to the creep parameter (Cuffey and Paterson 2010; Maussion et al. 2019). $A_{opt}$ can be found through a cross-validation method described in Pelto et al. (2019) and applied in Pelto et al. (2020).

The cross-validation approach for $A_{opt}$ requires direct observations of glacier ice thickness by employing Ice Penetrating Radar (IPR) techniques. Furthermore, Pelto et al. (2020) utilized IPR to measure the thickness of glaciers that had previously been estimated with inversion models and found, on average, a 38% difference in modelled and measured ice thickness. For watershed scale modelling, refined accuracy of ice thickness is critical; therefore, IPR measurements from two representative glaciers within the Adams watershed will be integrated into the OGGM model estimate to calibrate ice thickness measurements. To integrate measured ice thickness with modelled ice thickness, a minimized mean absolute error (MAE) approach is followed as outlined by Pelto et al. (2020) using the equation:

$$MAE = \frac{\sum_1^n |(H_{obs} - H_{mod})|}{n}$$ [ *Equation 6* ]

where $n$ is the number of grid cells where both gridded measurements of ice thickness ($H_{obs}$) and OGGM modelled estimates ($H_{mod}$) exist.

### 3.2.5 OGGM Ice Dynamics Modelling

The ice dynamics module in OGGM allows us to evolve glaciers within the Adams watershed over a set timeframe to assess the total volume of ice lost and remaining given certain climate scenarios. The revised AR6 report IPCC Climate Scenarios will force the extent and rate of glacier change within the watershed by altering glacier temperature sensitivities (IPCC 2021). The glacier runoff contribution to the Adams watershed is then estimated from the rate of annual ice volume change. The numerical solver utilized in the OGGM to model ice dynamics can account for any bed topography shape with high accuracy, except for areas of very steep slopes (Maussion et al. 2019). For any glaciated areas with very steep slopes in the Adams watershed, a diffusivity equation solver may need to be integrated into the computations (Jarosch et al. 2013).

## 3.3 Ice Penetrating Radar

Ice Penetrating Radar (IPR) is a well-established geophysical method for measuring ice thickness (Bogorodsky et al. 1985). Recent advents in technology have led to the development of lightweight systems (>10kg) that are readily transportable and suited for field operation on complex glacier terrain of modest extent (Mingo and Flowers 2010). These systems have been successful in measuring the thickness of Canadian polythermal glaciers to ~220m in depth and Icelandic temperate glaciers to ~ 550m in depth (Mingo and Flowers 2010). One transmitting unit and one receiving unit, equipped with a built in GPS, is pulled across the glacier surface and a recorded wavelength is measured approximately every 3-5 m along the route (Pelto et al. 2020). The frequency of the radar transmission can be altered for deeper glaciers by altering the length of the output and receiving antennae; however, for the purpose of this study, the default 520 Hz transmission with dipole antennas of 4m each (transmitting and receiving) is suitable (Mingo and Flowers 2010; Pelto et al. 2020). The IPR measurements in the Adams watershed will be conducted in May of 2024, using a Blue Systems Integration system. May is the safest time for traversing glaciers within the area, as the accumulated winter snow will condense and form stable snow bridges over crevasses. Measurements will be collected by traversing the glacier along set longitudinal cross profiles while maintaining a safe route. Raw data will be processed using the *irlib* open source package in Python and integrated into the OGGM model (Pelto et al. 2020).

# 4. Timeline

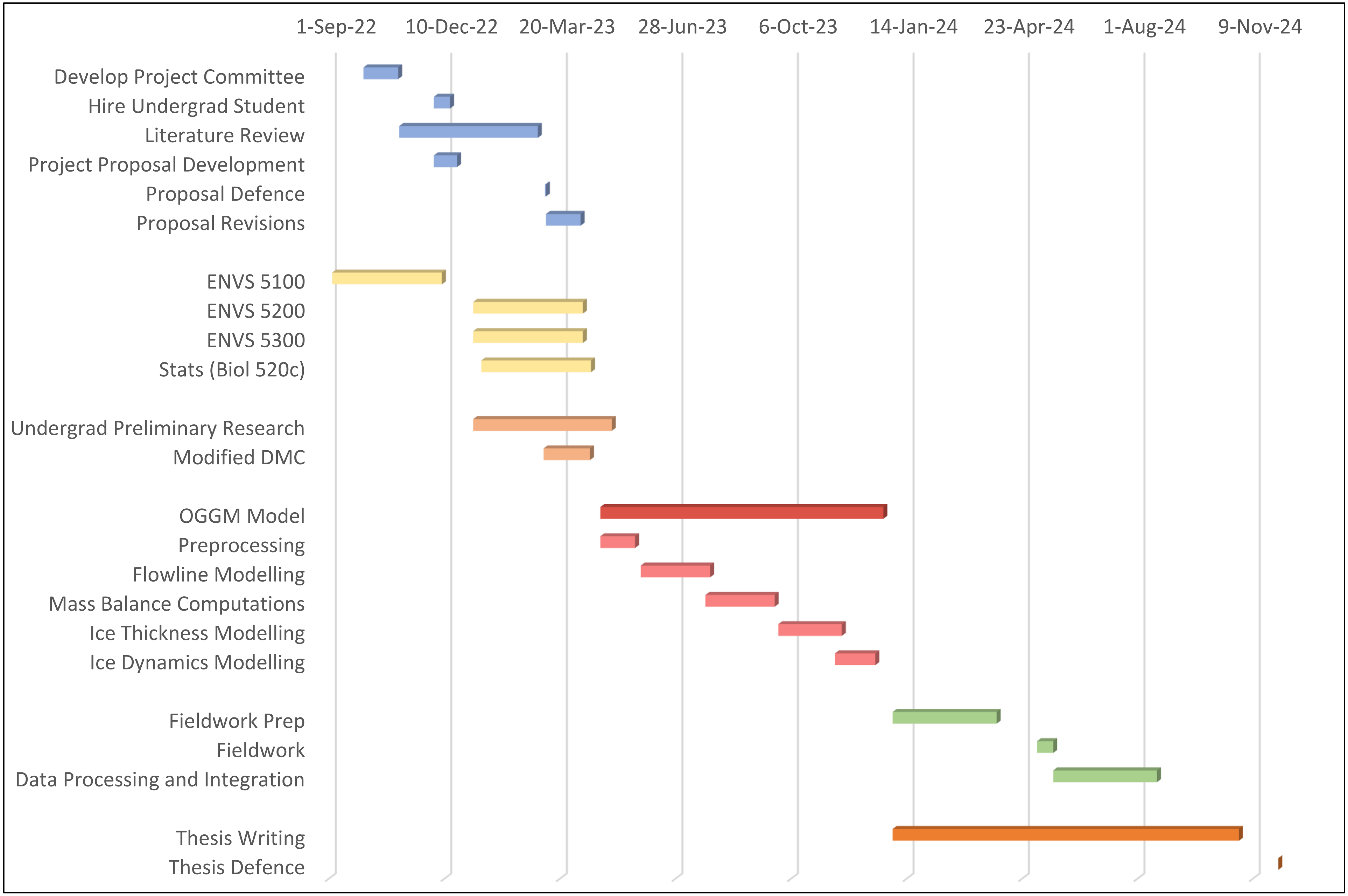
1-Sep-22
10-Dec-22
20-Mar-23
28-Jun-23
6-Oct-23
14-Jan-24
23-Apr-24
1-Aug-24
9-Nov-24
Develop Project Committee
Hire Undergrad Student
Literature Review
Project Proposal Development
Proposal Defence
Proposal Revisions
ENVS 5100
ENVS 5200
ENVS 5300
Stats (Biol 520c)
Undergrad Preliminary Research
Modified DMC
OGGM Model
Preprocessing
Flowline Modelling
Mass Balance Computations
Ice Thickness Modelling
Ice Dynamics Modelling
Fieldwork Prep
Fieldwork
Data Processing and Integration
Thesis Writing
Thesis Defence

# 5. Budget

This 2.5-year project will be funded through an NSERC research grant ($19,500 over two years) and the Shuswap Watershed Council ($8,000 over two years). Additionally, we are waiting to hear about a Mitacs Accelerate grant in partnership with Adams Lake Indian Band ($15,000 over two years). The secured funds will cover my stipend, any field equipment required, cost for a glacier travel professional, conference costs, and transportation to and from the glaciers (Table 1). Applications for conference cost reimbursements will also be submitted to the TRU Student Union to maximize funding from external sources.

*Table 1. Expenses for year 1 and 2 of the TRU Adams watershed glacier research project.*

| Expenses | | |
|---|---|---|
| Year 1 | Research stipend | $19,500 |
| | Conference expenses<br>International (Bosnia)<br>Local (BC) | $3,000 |
| | Tech equipment & software | $1,500 |
| | High resolution imagery | $1,000 |
| | Year 1 Total | $25,500 |
| | | |
| Year 2 | Research stipend | $19,500 |
| | Helicopter time | $8,000 |
| | Glacier safety professional | $1,500 |
| | Ice Penetrating Radar | $5,000 |
| | Field equipment | $1,000 |
| | Conference expenses | $500 |
| | Year 2 Total | $35,500 |

# 5. References


Arendt AA, Echelmeyer KA, Harrison WD, Lingle CS, Valentine VB. 2002. Rapid wastage of Alaska glaciers and their contribution to rising sea level. Science. 297(5580):382–386. doi:10.1126/SCIENCE.1072497. [accessed 2023 Feb 24]. https://pubmed.ncbi.nlm.nih.gov/12130781/.

Arrhenius S. 1896. On the influence of carbonic acid in the air upon the temperature of the ground. Philisophical Mag. 5(41):237–276.

Arrhenius S. 1908. Worlds in the Making; The Evolution of the Universe. New York: Harper & Brothers..

Barry RG. 2016. The status of research on glaciers and global glacier recession: a review: Prog Phys Geogr Earth Environ. 30(3):285–306. doi:10.1191/0309133306PP478RA. [accessed 2022 Sep 8]. https://journals.sagepub.com/doi/10.1191/0309133306pp478ra.

Barry RG, Gan TY. 2022. The Global Cryosphere: Past, Present, and Future. Second Edi. Cambridge, United Kingdom: Cambridge University Press.

Bevington AR, Menounos B. 2022. Accelerated change in the glaciated environments of western Canada revealed through trend analysis of optical satellite imagery. Remote Sens Environ. 270:112862. doi:10.1016/J.RSE.2021.112862.

Blunden J, Boyer T. 2021. State of the Climate in 2020. Bull Am Meteorol Soc. 102(8):S1–S475. doi:10.1175/2021BAMSSTATEOFTHECLIMATE.1. [accessed 2022 Dec 28]. https://journals.ametsoc.org/view/journals/bams/102/8/2021BAMSStateoftheClimate.1.xml.

Bogorodsky V V., Bentley CR, Gudmandsen PE. 1985. Radioglaciology. In: Glaciology and Quaternary Geology. Vol. 1. Dordrecht: Springer Netherlands. (Glaciology and Quaternary Geology). [accessed 2023 Feb 15]. http://link.springer.com/10.1007/978-94-009-5275-1.

Bolch T, Menounos B, Wheate R. 2010. Landsat-based inventory of glaciers in western Canada, 1985–2005. Remote Sens Environ. 114(1):127–137. doi:10.1016/J.RSE.2009.08.015.

Box GEP, Tiao GC. 1975. Intervention Analysis with Applications to Economic and Environmental Problems. J Am Stat Assoc. 70(349):70–79. doi:10.1080/01621459.1975.10480264.

Campbell GS, Norman JM. 1998. An Introduction to Environmental Biophysics.

Chesnokova A, Baraër M, Laperrière-Robillard T, Huh K. 2020. Linking Mountain Glacier Retreat and Hydrological Changes in Southwestern Yukon. Water Resour Res. 56(1):e2019WR025706. doi:10.1029/2019WR025706. [accessed 2022 Sep 20]. https://onlinelibrary.wiley.com/doi/full/10.1029/2019WR025706.

Clarke GKC, Jarosch AH, Anslow FS, Radić V, Menounos B. 2015. Projected deglaciation of western Canada in the twenty-first century. Nat Geosci. 8(5). doi:10.1038/ngeo2407.

Cogley JG, Hock R, Rasmussen LA, Arendt AA, Bauder A, Braithwaite RJ, Jansson P, Kaser G, Möller M, Nicholson L, et al. 2011. Glossary of Glacier Mass Balance and Related Terms. Arctic, Antarct Alp Res. 44(2):256–258. doi:10.1657/1938-4246-44.2.256B. [accessed 2023 Feb 22]. https://www.tandfonline.com/doi/abs/10.1657/1938-4246-44.2.256b.

Cuffey KM, Paterson WSB. 2010. The physics of glaciers. Fourth. Academic Press.

DFO. 2022 Aug. BC Salmon Restoration Fund project overviews. Gov Canada Dep Fish Ocean.:1. [accessed 2023 Feb 22]. https://www.dfo-mpo.gc.ca/fisheries-peches/initiatives/fish-fund-bc-fonds-peche-cb/projects-projets-eng.html.

Farinotti D, Brinkerhoff DJ, Clarke GKC, Fürst JJ, Frey H, Gantayat P, Gillet-Chaulet F, Girard C, Huss M, Leclercq PW, et al. 2017. How accurate are estimates of glacier ice thickness? Results from ITMIX, the Ice Thickness Models Intercomparison eXperiment. Cryosphere. 11(2):949–970. doi:10.5194/TC-11-949-2017.

Glen J. 1955. The creep of polycrystalline ice. Mater Sci. 228(1175):519–538. doi:10.1098/RSPA.1955.0066.

GovBC. 2022. Single Waterbody Query: Adams Lake. Gov BC Minist Environ Fish Invent Data Queries. [accessed 2023 Feb 22]. https://a100.gov.bc.ca/pub/fidq/infoSingleWaterbody.do.

[GovCan] Government of Canada. 2022a. Blue River Canadian Climate Normals 1981-2010 Station Data. Environ Canada. [accessed 2023 Jan 4]. https://climate.weather.gc.ca/climate_normals/results_1981_2010_e.html?stnID=1237&autofwd=1.

[GovCan] Government of Canada. 2022b. Celista Canadian Climate Normals 1981-2010 Station Data. Environ Canada. [accessed 2023 Jan 4]. https://climate.weather.gc.ca/climate_normals/results_1981_2010_e.html?stnID=1247&autofwd=1.

Hargreaves GH, Samani ZA. 1982. Estimating potential evapotranspiration. J Irrig Drain Div - ASCE. 108(IR3). doi:10.1061/taceat.0008673.

Harris I, Osborn TJ, Jones P, Lister D. 2020. Version 4 of the CRU TS monthly high-resolution gridded multivariate climate dataset. Sci data. 7(1). doi:10.1038/S41597-020-0453-3. [accessed 2023 Feb 28]. https://pubmed.ncbi.nlm.nih.gov/32246091/.

Henderson MA, Levy DA, Stockner JS. 1992. Probable consequences of climate change on freshwater production of Adams River sockeye salmon (Oncorynchus nerka). GeoJournal. 28(1). doi:10.1007/BF00216406.

Holmes D, Arnouse C. 2021. ALIB Nutrient Supplementation Program. Adams Lake Band Press Release.:1. https://adamslakeband.org/wp-content/uploads/2021/01/ALIB-Adams-RIver-Salmon-Restoration-Press-Release-Jan-12-2021.pdf.

Hugonnet R, McNabb R, Berthier E, Menounos B, Nuth C, Girod L, Farinotti D, Huss M, Dussaillant I, Brun F, et al. 2021. Accelerated global glacier mass loss in the early twenty-first century. Nature. 592(7856). doi:10.1038/s41586-021-03436-z.

Hume JM., Morton KF, Lofthouse D, MacKinlay D, Shortreed KS, Grout J, Volk E. 2003. Evaluation of Restoration Efforts on the 1996 Upper Adams River sockeye salmon run. Cultus Lake, BC. [accessed 2022 Oct 6]. https://www.researchgate.net/publication/251998136_Evaluation_of_Restoration_Efforts_on_the_1996_Upper_Adams_River_sockeye_salmon_run/figures.

Huss M, Jouvet G, Farinotti D, Bauder A. 2010. Future high-mountain hydrology: A new parameterization of glacier retreat. Hydrol Earth Syst Sci. 14(5). doi:10.5194/hess-14-815-2010.

Hutter K. 1983. Material Science of Ice and the Mechanics of Glaciers and Ice Sheets. In: Theoretical Glaciology. Vol. 1. Springer Netherlands.

IPCC. 2021. Summary for Policymakers. In: Climate Change. 2021. The Physical Science Basis. Contribution of Working Group I to the Sixth Assessment Report of the Intergovernmental Panel on Climate Change [Masson-Delmotte, V., P. Zhai, A. Pirani, S.L. Connors, C. Péan, S. Berger, N. Caud, Y. Chen, L. Goldfarb, M.I. Gomis, M. Huang, K. Leitzell, E. Lonnoy, J.B.R. Matthews, T.K. Maycock, T. Waterfield, O. Yelekçi, R. Yu, and B. Zhou (eds.)]. Cambridge University Press, Cambridge, United Kingdom and New York, NY, USA, pp. 3−32, doi:10.1017/9781009157896.001.

Jacob T, Wahr J, Pfeffer WT, Swenson S. 2012. Recent contributions of glaciers and ice caps to sea level rise. Nat 2012 4827386. 482(7386):514–518. doi:10.1038/nature10847. [accessed 2023 Feb 28]. https://www.nature.com/articles/nature10847.

Jansson P, Hock R, Schneider T. 2003. The concept of glacier storage: a review. J Hydrol. 282(1–4):116–129. doi:10.1016/S0022-1694(03)00258-0.

Jarosch AH, Schoof CG, Anslow FS. 2013. Restoring mass conservation to shallow ice flow models over complex terrain. Cryosph. 7(1):229–240. doi:10.5194/TC-7-229-2013.

Jarvis A, Guevara E, Reuter HI, Nelson AD. 2008. Hole-filled SRTM for the globe : version 4 : data grid. CGIAR Consort Spat Inf. [accessed 2023 Feb 28]. http://srtm.csi.cgiar.org/.

Kargel J, Leonard G, Bishop M, Kääb A, Raup B. 2014. Global Land Ice Measurements from Space. Kargel J, Leonard G, Bishop M, Kääb A, Raup B, editors. Springer Berlin Heidelberg.

Kienholz C, Rich JL, Arendt AA, Hock R. 2014. A new method for deriving glacier centerlines applied to glaciers in Alaska and northwest Canada. Cryosphere. 8(2):503–519. doi:10.5194/TC-8-503-2014.

Kruger M, Saayman M. 2017. An experience-based typology for natural event tourists. Int J Tour Res. 19(5):605–617. doi:10.1002/JTR.2133.

Li Q, Wei X, Zhang M, Liu W, Giles-Hansen K, Wang Y. 2018. The cumulative effects of forest disturbance and climate variability on streamflow components in a large forest-dominated watershed. J Hydrol. 557:448–459. doi:10.1016/J.JHYDROL.2017.12.056.

Maussion F, Butenko A, Champollion N, Dusch M, Eis J, Fourteau K, Gregor P, Jarosch AH, Landmann J, Oesterle F, et al. 2019. The Open Global Glacier Model (OGGM) v1.1. Geosci Model Dev. 12(3). doi:10.5194/gmd-12-909-2019.

Milner AM, Brown LE, Hannah DM. 2009. Hydroecological response of river systems to shrinking glaciers. Hydrol Process. 23(1):62–77. doi:10.1002/HYP.7197. [accessed 2022 Sep 20]. https://onlinelibrary.wiley.com/doi/full/10.1002/hyp.7197.

Mingo L, Flowers GE. 2010. An integrated lightweight ice-penetrating radar system. J Glaciol. 56(198). doi:10.3189/002214310793146179.

Moore RD, Fleming SW, Menounos B, Wheate R, Fountain A, Stahl K, Holm K, Jakob M. 2009. Glacier change in western North America: influences on hydrology, geomorphic hazards and water quality. Hydrol Process. 23(1):42–61. doi:10.1002/HYP.7162. [accessed 2022 Sep 21]. https://onlinelibrary-wiley-com.ezproxy.tru.ca/doi/full/10.1002/hyp.7162.

Pelto BM, Maussion F, Menounos B, Radić V, Zeuner M. 2020. Bias-corrected estimates of glacier thickness in the Columbia River Basin, Canada. J Glaciol. 66(260):1051–1063. doi:10.1017/JOG.2020.75.

Pelto BM, Menounos B, Marshall SJ. 2019. Multi-year evaluation of airborne geodetic surveys to estimate seasonal mass balance, Columbia and Rocky Mountains, Canada. Cryosphere. 13(6):1709–1727. doi:10.5194/TC-13-1709-2019.

Pfeffer WT, Arendt AA, Bliss A, Bolch T, Cogley JG, Gardner AS, Hagen JO, Hock R, Kaser G, Kienholz C, et al. 2014. The randolph glacier inventory: A globally complete inventory of glaciers. J Glaciol. 60(221):537–552. doi:10.3189/2014JOG13J176.

Pike RG, Redding TE, Moore D, Winkler RD, Bladon KD. 2010. Compendium of Forest Hydrology and Geomorphology in British Columbia Volume 1 of 2. Victoria. [accessed 2021 Nov 26]. www.publications.gov.bc.ca.

Pitman KJ, Moore JW, Sloat MR, Beaudreau AH, Bidlack AL, Brenner RE, Hood EW, Pess GR, Mantua NJ, Milner AM, et al. 2020. Glacier Retreat and Pacific Salmon. Bioscience. 70(3):220–236. doi:10.1093/BIOSCI/BIAA015. [accessed 2022 Sep 20]. https://academic.oup.com/bioscience/article/70/3/220/5799047.

Pradhananga D, Pomeroy JW. 2022. Recent hydrological response of glaciers in the Canadian Rockies to changing climate and glacier configuration. Hydrol Earth Syst Sci. 26(10):2605–2616. doi:10.5194/HESS-26-2605-2022. [accessed 2022 Sep 7]. https://hess.copernicus.org/articles/26/2605/2022/.

Rodionov S. 2005. A Brief Overview of the Regime Shift Detection Methods. Large-Scale Disturbances (Regime Shifts) Recover Aquat Syst Challenges Manag Towar Sustain.(Table 4).

Rounce DR, Hock R, Maussion F, Hugonnet R, Kochtitzky W, Huss M, Berthier E, Brinkerhoff D, Compagno L, Copland L, et al. 2023. Global glacier change in the 21st century: Every increase in temperature matters. Science (80- ). 379(6627):78–83. doi:10.1126/SCIENCE.ABO1324. [accessed 2023 Jan 10]. https://www-science-org.ezproxy.tru.ca/doi/10.1126/science.abo1324.

Searcy JK, Hardison CH. 1960. Double-Mass Curves. Washington, DC: Geological Survey. US Department of the Interior. .

Spehn E, Berge E, Bugmann H, Groombridge B, Hamilton L, Hofer T, Ives J, Jodha N, Messerli B, Pratt J, et al. 2002. Mountain Systems. In: Fitzharris B, Shrestha K, editors. Mountain Biodiversity: A Global Assessment. Vol. 1. 1st ed. Washington DC: Island Press. p. 681–716.

Stahl K, Moore RD. 2006. Influence of watershed glacier coverage on summer streamflow in British Columbia, Canada. Water Resour Res. 42(6):6201. doi:10.1029/2006WR005022. [accessed 2022 Sep 29]. https://onlinelibrary.wiley.com/doi/full/10.1029/2006WR005022.

Wei WWS. 2006. Time Series Analysis: Univariate and Multivariate Methods Second Edition. Pearson Educ Inc. SFB 373(Chapter 5):837–900. [accessed 2023 Feb 28]. http://books.google.com.au/books?id=B8_1UBmqVUoC.

Wei X, Zhang M. 2010. Quantifying streamflow change caused by forest disturbance at a large spatial scale: A single watershed study. Water Resour Res. 46(12):12525. doi:10.1029/2010WR009250. [accessed 2023 Feb 14]. https://onlinelibrary.wiley.com/doi/full/10.1029/2010WR009250.

WGMS. 2021. Global Glacier Change Bulletin No. 4 (2018–2019). Zemp, M., Nussbaumer, S.U., GärtnerRoer, I., Bannwart, J., Paul, F., and Hoelzle, M. (eds.), ISC (WDS)/ IUGG (IACS)/ UNEP/ UNESCO/ WMO, World Glacier Monitoring Service, Zurich, Switzerland, 278 pp., publication based on database version: doi:10.5904/wgms-fog-2021-05.

Winkler RD, Moore RD, Redding Todd E, Spittlehouse DL, Smerdon B. 2010. The Effects of Forest Disturbance on Hydrologic Processes and Watershed Response, Chapter 7. In: Pike RG, Redding T E, Moore RD, Winkler RD, Bladon KD, editors. Compendium of Forest Hydrology and Geomorphology in British Columbia. Victoria, BC: BC Ministry of Forests and Range. p. 179–202. [accessed 2020 Nov 20]. https://www.researchgate.net/publication/242541583_The_Effects_of_Forest_Disturbance_on_Hydrologic_Processes_and_Watershed_Response_Chapter_7.

Zemp M, Huss M, Thibert E, Eckert N, McNabb R, Huber J, Barandun M, Machguth H, Nussbaumer SU, Gärtner-Roer I, et al. 2019. Global glacier mass changes and their contributions to sea-level rise from 1961 to 2016. Nat 2019 5687752. 568(7752):382–386. doi:10.1038/s41586-019-1071-0. [accessed 2022 Dec 28]. https://www.nature.com/articles/s41586-019-1071-0.

Zhang L, Dawes WR, Walker GR. 2001. Response of mean annual evapotranspiration to vegetation changes at catchment scale. Water Resour Res. 37(3):701–708. doi:10.1029/2000WR900325. [accessed 2023 Feb 28]. https://onlinelibrary.wiley.com/doi/full/10.1029/2000WR900325.

# 6. Appendix

Appendix A. Map of the 10 major drainage basins in BC.

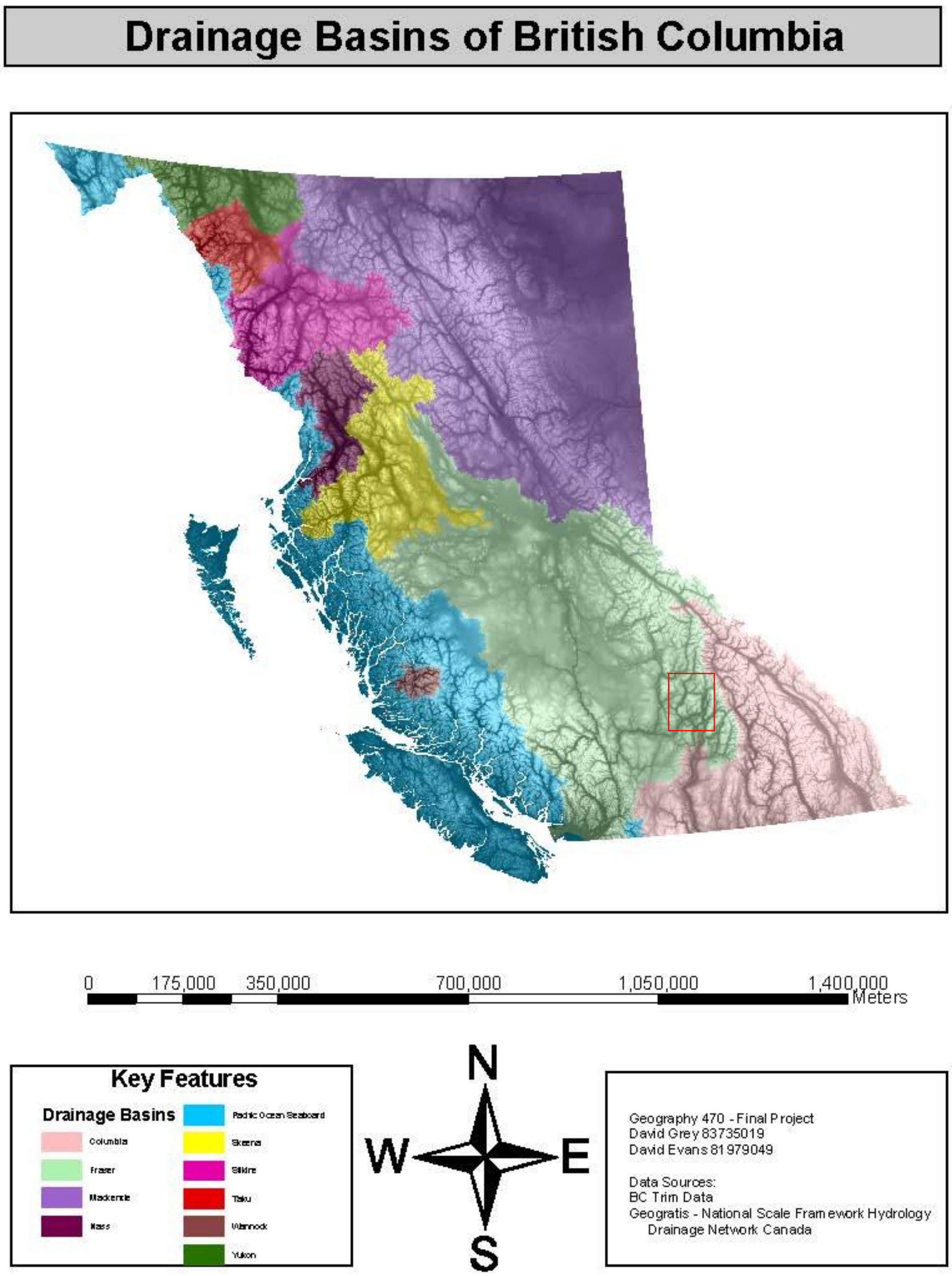

Appendix B. Upper Adams watershed Canadian Climate Normals from 1981 – 2010.

| **Station** | Blue River A |
|---|---|
| **Coordinates** | 52°07'44.500" N<br>119°17'22.300" W |
| **Elevation** | 690.4 m |

| | **Jan** | **Feb** | **Mar** | **Apr** | **May** | **Jun** | **Jul** | **Aug** | **Sep** | **Oct** | **Nov** | **Dec** |
|---|---|---|---|---|---|---|---|---|---|---|---|---|
| **Temperature** | | | | | | | | | | | | |
| Daily Average (°C) | -7.3 | -4.4 | 0.5 | 5.2 | 10.2 | 14 | 16.4 | 16 | 11 | 4.5 | -1.9 | -7.1 |
| Daily Maximum (°C) | -3.5 | 0.4 | 6.1 | 11.9 | 17.6 | 21.1 | 24 | 24.2 | 18.3 | 9.2 | 0.9 | -3.7 |
| Daily Minimum (°C) | -11 | -9.1 | -5.2 | -1.6 | 2.8 | 6.9 | 8.8 | 7.7 | 3.7 | -0.2 | -4.6 | -10.5 |
| Extreme Maximum (°C) | 8.6 | 11 | 19.4 | 28 | 33 | 34.1 | 37.5 | 37.8 | 33.6 | 25.5 | 16.1 | 10 |
| Extreme Minimum (°C) | -44 | -37.8 | -30 | -15.6 | -6.8 | -2.7 | -0.6 | -3.5 | -7.2 | -20 | -36.9 | -44.8 |

| **Precipitation** | | | | | | | | | | | | | Annual Total |
|---|---|---|---|---|---|---|---|---|---|---|---|---|---|
| Rainfall (mm) | 21.3 | 17.6 | 35.8 | 52.7 | 75.6 | 98.8 | 107.3 | 82.4 | 71.3 | 94 | 49.5 | 13.5 | 719.7 |
| Snowfall (cm) | 113.5 | 49.5 | 38.3 | 7 | 0.4 | 0 | 0 | 0 | 0 | 10 | 82.4 | 103.4 | 404.4 |
| Precipitation (mm) | 105.4 | 53.8 | 64.7 | 58.7 | 75.8 | 98.8 | 107.3 | 82.4 | 71.3 | 102.5 | 115.2 | 88.4 | 1024.4 |

Appendix C. Lower Adams watershed Canadian Climate Normals from 1981 – 2010.

| | |
|---|---|
| **Station** | Celista |
| **Coordinates** | 50°57'20.000" N<br>119°22'46.000" W |
| **Elevation** | 515.0 m |

| | **Jan** | **Feb** | **Mar** | **Apr** | **May** | **Jun** | **Jul** | **Aug** | **Sep** | **Oct** | **Nov** | **Dec** |
|---|---|---|---|---|---|---|---|---|---|---|---|---|
| **Temperature** | | | | | | | | | | | | |
| Daily Average (°C) | -3.8 | -2.5 | 2 | 7.7 | 12.1 | 15.7 | 18.5 | 17.9 | 12.7 | 6 | 0.8 | -3.1 |
| Daily Maximum (°C) | -1.1 | 1.3 | 6.8 | 14 | 18.7 | 22.4 | 25.8 | 25.4 | 19.3 | 10.3 | 3.4 | -0.7 |
| Daily Minimum (°C) | -6.6 | -6.2 | -2.9 | 1.4 | 5.5 | 9 | 11.2 | 10.4 | 6.2 | 1.6 | -1.9 | -5.4 |
| Extreme Maximum (°C) | 13 | 12 | 20 | 26 | 32 | 37 | 37 | 37.5 | 32 | 22 | 15 | 8 |
| Extreme Minimum (°C) | -29 | -29 | -19 | -8 | -3 | -1 | 5 | 3 | -2 | -14 | -19.5 | -32 |

| **Precipitation** | | | | | | | | | | | | | Annual Total |
|---|---|---|---|---|---|---|---|---|---|---|---|---|---|
| Rainfall (mm) | 18.3 | 17.9 | 30.5 | 41.8 | 64.4 | 65.9 | 53.7 | 46 | 43.3 | 61.8 | 53 | 18.7 | 515.3 |
| Snowfall (cm) | 66.3 | 24.9 | 15 | 0.2 | 0 | 0 | 0 | 0 | 0 | 0.6 | 37.5 | 79.3 | 223.8 |
| Precipitation (mm) | 84.7 | 42.9 | 45.5 | 42 | 64.4 | 65.9 | 53.7 | 46 | 43.3 | 62.4 | 90.4 | 98 | 739.1 |